



# Infrared Contrast Enhancement Through Log-Power Histogram Modification

**Alexander Toet**

*TNO, Kampweg 5, 3769DE, Soesterberg, The Netherlands*

*alex.toet@tno.nl*

**Tirui Wu**

*Ford Motor Research & Engineering (Nanjing) Co., Ltd, Nanjing, China*

*tiruiwu@gmail.com*

## Abstract

A simple power-logarithm histogram modification operator is proposed to enhance infrared (IR) image contrast. The algorithm combines a logarithm operator that smoothes the input image histogram while retaining the relative ordering of the original bins, with a power operator that restores the smoothed histogram to an approximation of the original input histogram. Contrast enhancement is achieved by using the cumulative distribution function of the resulting histogram in a standard lookup table based histogram equalization procedure. The method is simple and independent of image content, and (unlike most existing contrast enhancement algorithms) does not suffer from the occurrence of artifacts, over-enhancement and unnatural effects in the processed images. The method can be applied both in a direct (DPL) and in an iterative (IPL) mode. Objective (computational) and subjective (visual) evaluation studies using a wide range of different IR input images showed that DPL and IPL both significantly enhance image contrast while retaining the overall image structure and preserving the perceptibility of small details and targets. DPL retains image structure slightly better than IPL, while IPL enhances contrast slightly more than DPL. Experimental results proved that the proposed method is a robust and efficient technique for effective IR image contrast enhancement.

**Keywords:** infrared image enhancement; contrast enhancement; histogram modification; pow-log operation

## 1. Introduction

Infrared imagery is widely used in military, civilian, scientific and medical areas. However, infrared (IR) images are typically degraded due to noise, low contrast (since IR image sensors cannot clearly distinguish objects from their backgrounds if they have a similar emissivity) and blur (due to the inhomogeneous photosensitive response of infrared detector and non-ideal optics system). Effective contrast enhancement algorithms are therefore essential to improve the visibility of IR imagery.

A broad range of contrast enhancement algorithms is currently available (for recent reviews of the state-of-the-art of contrast enhancement techniques see e.g. [1–4]. Methods such as graylevel transformation techniques (e.g., logarithm, power-law and piecewise linear transformations [5–7]) and histogram based processing techniques (e.g., histogram equalization, histogram specification [7]) are well known and widely deployed to enhance image contrast. However, most of these techniques are inappropriate to enhance IR images since they were developed for use in the visual spectral domain and therefore do not take the characteristics of IR imagery into account [8].

IR images are typically distinct from images registered in the visual spectral domain. For instance, the visibility of targets near the horizon may be significantly reduced due to a large difference in radiance between ground and sky or sea (horizon effect), while image variations over large areas with a homogeneous temperature distribution often represent

noise. In addition, small and warm objects (such as engines or living beings) typically appear with excessive contrast and may be saturated. To effectively enhance IR image contrast methods are therefore required that enhance the global contrast and perceptibility of details without highlighting the noise and introducing unwanted artifacts.

This section presents a brief overview of existing approaches to contrast enhancement. Recent and more extensive reviews of the state-of-the-art of contrast enhancement techniques for image enhancement in general [1–4] and for IR image enhancement in particular [8, 9] can be found elsewhere.

Traditional global histogram equalization (HE) uses the histogram of the entire input image as its transformation function [7]. Global histogram equalization is simple and effective, but its effect is typically too severe for IR image enhancement since it results in the over-enhancement (introduction of noise) in the background and a contrast deterioration of small targets.

Figure 1a shows a medical image with a large dark background. Histogram equalization fails to improve contrast for this image (Fig. 1b) since its graylevel distribution (Fig. 1d) is extremely peaked (i.e. a single histogram component - representing the dark image background - accounts for a large percentage of the total distribution). The spike in the input histogram causes a steep slope in the CDF which is used as the transformation function in the equalization process. As result a narrow range of low graylevel values is mapped onto a wide range of much larger values and the output image has a washed-out appearance, while its dynamic range becomes even smaller than that of the input image.

A wide range of adaptive and local variations of histogram equalization have been developed to overcome the limitations of HE [1, 2, 10, 11].

In adaptive (or block-overlapped [12]) histogram equalization (AHE) separate histograms are calculated for different image regions which are then used to redistribute the local graylevel values. A typical approach is to compute the histogram over a sliding rectangular window, use it to equalize the local graylevel distribution, and map the center pixel of the window region to its histogram equalized value using this function. The center of the rectangular region is then moved to the adjacent pixel and the histogram equalization is repeated. In a block-overlapped approach this procedure is repeated pixel by pixel for all input image pixels.

This method allows each pixel to adapt to its local neighborhood, so that high contrast can be obtained for all locations in the image. However, since local histogram equalization must be performed for all pixels in the entire image frame, the computational complexity is very high. To reduce this computational complexity and obtain the advantage of local adaptability of block-overlapped histogram equalization, sub-block non-overlapped histogram equalization can be applied. However, this non-overlapped method sometimes suffers from blocking effects. The use partially overlapping blocks combines the simplicity of global histogram equalization with the high contrast stretching capability of local histogram equalization [12].

Although AHE can achieve higher contrast enhancement than HE it can also give images a noisier appearance because homogeneous regions tend to become over-enhanced. A variant of adaptive histogram equalization called contrast limited adaptive histogram equalization (CLAHE [13]) prevents this by limiting the amplification. The contrast amplification in the vicinity of a given pixel value is proportional to the slope of the neighborhood CDF. CLAHE limits the amplification by clipping the histogram at a predefined value before computing

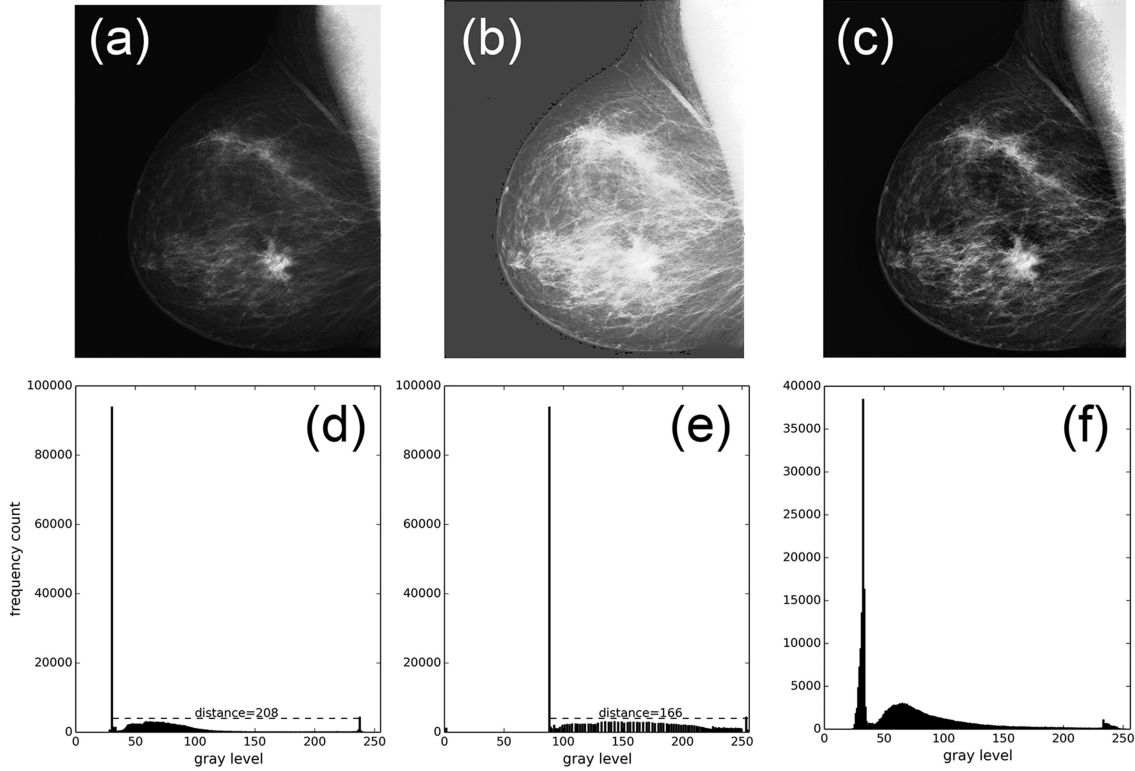


**Fig. 1:** Histogram equalization fails when the input image (a) has a large area low-intensity background. In this case the histogram (d) has a spike component corresponding to the background graylevel. After histogram equalization the output image (b) has a severe washed-out appearance while its dynamic range actually becomes smaller (e). CLAHE avoids over amplification by limiting the amount of contrast enhancement (c) and produces a histogram (f) that is more similar to the input one (d).

the CDF. This limits the slope of the CDF and therefore of the transformation function. of CLAHE.

Although CLAHE enhances the contrast of IR images better than HE (even in large low-contrast areas) it still tends to over-enhance contrast and produces unnatural looking images [8]. Adapted versions of clipped histogram equalization (CHE) have successfully been deployed to enhance the contrast of IR imagery [8], but a major drawback of this approach is the fact that the selection of the optimal transform parameters requires user intervention which makes the method less suitable for automatic systems [10].

Bi- or multi-histogram equalization (Bi-HE or Mu-HE) methods divide the histogram into two or more sub-histograms and individually equalize each sub-histogram [1, 2, 10]. The Brightness-preserving Bi-Histogram Equalization (BBHE) method uses the mean image intensity as the threshold value [14], while the Dualistic Sub-Image Histogram Equalization (DSIHE) method uses the median instead of the mean [15].

The Brightness-Preserving Histogram Equalization with Maximum Entropy (BPHEME) method preserves the brightness and also maximizes the entropy of the enhanced image via histogram specification [16]. To reduce the computational cost, Cascaded Multistep Binomial Filtering Histogram Equalization (CMBFHE) was utilized to achieve the same low-pass filter mask [17]. However, its time complexity is still much higher than BBHE and DSIHE.

The Recursive Sub-Image Histogram Equalization (RSIHE) method has the same time complexity, but extends DSIHE by including multi-equalizations to reduce the generation of artifacts [18]. In addition to histogram separation techniques, the Recursively Separated and Weighted Histogram Equalization (RSWHE) method uses a weighting function to smooth each sub-histogram for image enhancement and brightness preservation [19].

The Flattest Histogram Specification with Accurate Brightness Preservation (FHSABP) method utilizes convex optimization [20]. In order to concurrently apply traditional gamma correction techniques and HE, the Dynamic Contrast Ratio Gamma Correction (DCRGC) method directly applies the contrast ratio as a parameter [21]. However, it cannot be automatically generated. Bi-HE methods can significantly enhance image contrast and may preserve image brightness to some degree, but introduce undesirable artifacts. Multi-HE methods show better brightness preservation and prevent introduction of undesirable artifacts but may not sufficiently enhance contrast.

Recently several methods have been proposed to perform histogram modification (HM) prior to HE.

Gray-Level Grouping (GLG) first groups the histogram components of a low-contrast image into a proper number of bins according to a selected criterion, then redistributes these bins uniformly over the grayscale, and finally ungroups the previously grouped gray-levels [22]. Selective GLG can be used to selectively control the grouping of histogram components [23]. Since the resulting histogram is more uniform it is also more suitable as input for HE. Although GLG can effectively prevent over- and under- enhancement, it is computationally complex and may cause flicker when applied to video sequences.

Arici et al. [24] formulated HM in an optimization framework that minimizes a cost function to compute a modified target histogram. The cost function is composed of penalty terms of minimum histogram deviation from both the original and uniform histograms and histogram smoothness. Furthermore, edge information is embedded into the cost function to weigh pixels around region boundaries to address noise and black/white stretching. This approach can achieve different levels of contrast enhancement through the use of different adaptive parameters. This allows contrast enhancement of an image without introducing visual artifacts that decrease its visual quality or cause it to have an unnatural appearance. However, these parameters have to be manually tuned according to the image content to achieve high contrast. Also, the use of local variance information may cause a loss of information in homogeneous image regions.

Other techniques perform contrast enhancement in a transformed domain such as the Fourier transform [7], the DCT [25] or the pyramid and wavelet transforms [26]. Although these methods may achieve better results than HE they are usually complex and time consuming.

There are also contrast enhancement methods specifically intended for the application to IR images. Plateau histogram equalization employs a threshold value to constrain background noise while enhancing image contrast [27]. A drawback of this method is that image details represented with atypical graylevel values may be lost when they are merged with other graylevels. Double-plateau histogram equalization prevents this effect by using both an upper threshold value to constrain background noise and a lower threshold value to preserve image details. However, a critical issue with this method is the selection of threshold values. This problem can be addressed by adaptively calculating both thresholds [28]. The variational infrared image enhancement algorithm [31] employs gradient field equalization in combination with adaptive dual thresholds to prevent over-enhancement and achieves noise

suppression through minimization of the total variation in the reconstructed image. Other methods for IR contrast enhancement include the use of a multiscale top-hat transform [30] and multi-scale saliency maps [31].

In this paper we propose a power-logarithm operator to modify the histogram of IR images prior to HE. The method effectively enhances the contrast of IR images and is independent of image content. It is simple, can be applied both in a direct or iterative mode, and (unlike most existing contrast enhancement algorithms) does not suffer from the occurrence of artifacts, over-enhancement and unnatural effects in the processed images.

This paper is structured as follows. Section 2 presents two implementations of the new image enhancement method. Section 3 describes the methods used to perform both an objective and subjective evaluation of the effectiveness of the newly proposed method. Section 4 presents the results of the evaluation study and compares the performance of the proposed method with the performance of the popular HE and CLAHE contrast enhancement techniques. The conclusions of this study are presented in Section 5.

## 2. Pow-Log Contrast Enhancement

### 2.1 The Pow-Log Operator

As discussed above standard HE fails to increase contrast when the image histogram contains large spikes. Hence we need a monotonously increasing function (i.e. a function that retains the relative size ordering of the histogram bins) that effectively reduces the effects of spikes. A simple combination of a power and logarithm (pow-log) operator satisfies this requirement:

$$h'[i] = \text{pow}(\log(h[i] + \alpha), \beta), \quad 0 \leq i \leq L - 1, \quad \alpha > 1 \quad (1)$$

where

- $h$  and  $h'$  represent respectively the original and modified histograms,
- $\alpha$  is a number larger than 1 introduced to avoid taking the logarithm of zero for empty histogram bins,
- $\beta$  is the exponent of the power function, and
- $L$  is the number of available graylevels.

The log transformation serves to compress the dynamic range of the input histogram by compressing large values and expanding small values, and effectively reduces the relative contribution of spikes in the histogram. The power transform has the inverse effect: it expands larger values relative to smaller values. The power transform partly restores the histogram to its original shape. The overall pow-log function yields a smoothed version of the original histogram in which the relative contribution of spikes has been diminished. Fig. 2 illustrates the effect of this operator on the medical image from Fig. 1a.

### 2.2 Direct Mode

When directly applied the pow-log operator (Direct Pow-Log or DPL) redistributes the original image histogram and image contrast is enhanced by using the cumulative distribution function of the resulting histogram in a standard lookup table based histogram equalization procedure. This approach requires the selection of a value for  $\beta$ : if  $\beta$  is too small there will be no appreciable contrast enhancement; if  $\beta$  is too large the transformation will suffer from the same problems as HE (washout; see Fig. 3).

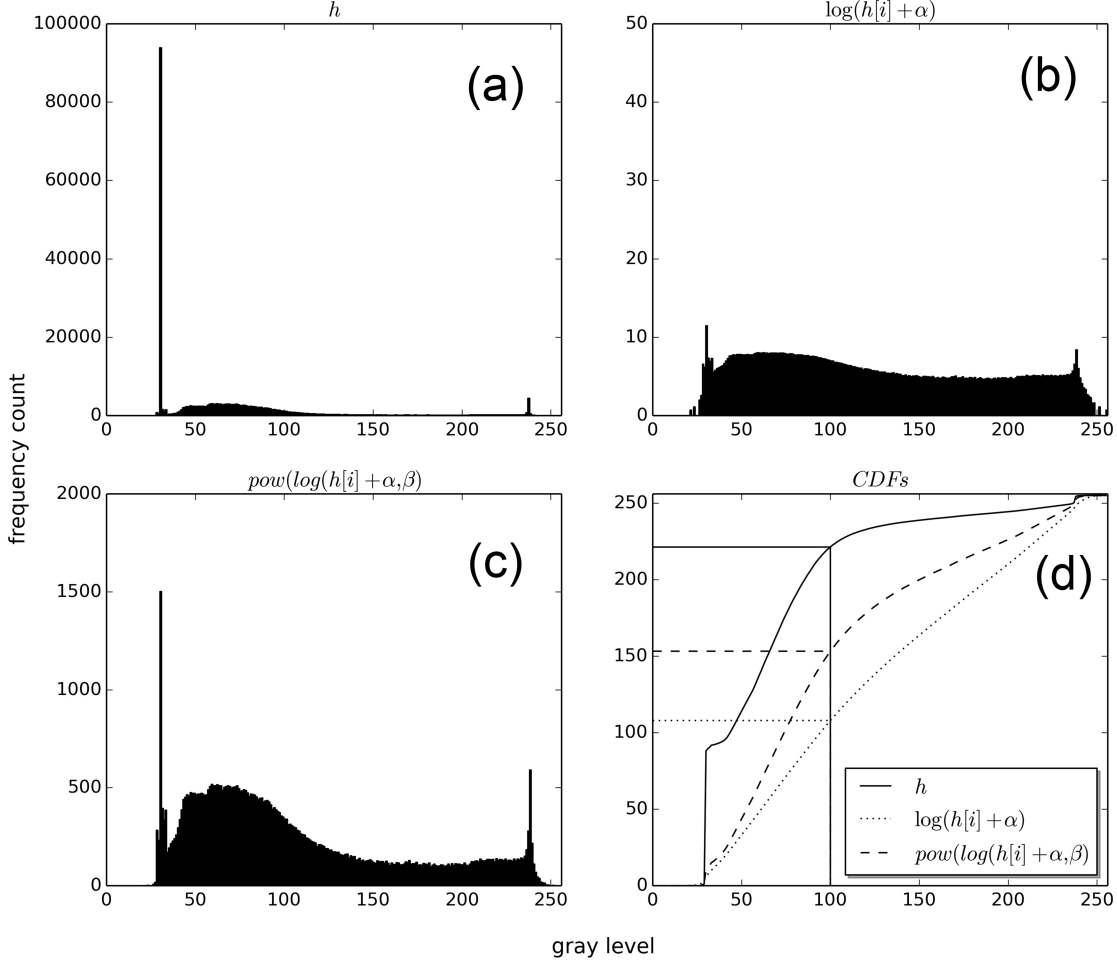


**Fig. 2:** Effect of the pow-log contrast operator. (a) The original distribution has a large peak representing the dark background. (b) The logarithm operator reduces this large spike and makes the distribution more uniform. (c) The power operator restores the distribution to one that is similar to the original distribution.

Arici et al. [24] showed that the optimally enhanced (in the sense that contrast is enhanced while mean brightness is preserved and the introduction of visual artifacts is prevented) distribution is a linear combination of the original and the uniform distribution:

$$h_o = \frac{1}{1+\lambda} h_i + \frac{\lambda}{1+\lambda} h_u \quad (2)$$

where  $h_i$ ,  $h_o$  and  $h_u$  are respectively the input, output and uniform histograms, and  $\lambda$  is used to control the degree of enhancement. When  $\lambda$  is small the output histogram is nearly equal to the input histogram, while it approaches the uniform histogram when  $\lambda$  is large. Hence, the optimal value of  $\beta$  can automatically be obtained by means of a simple heuristic search process: find the value of  $\beta$  that satisfies

$$\beta = \arg \max(\text{cross\_corellation}(h_o, h_i) + \text{cross\_corellation}(h_o, h'_i)) \quad (3)$$

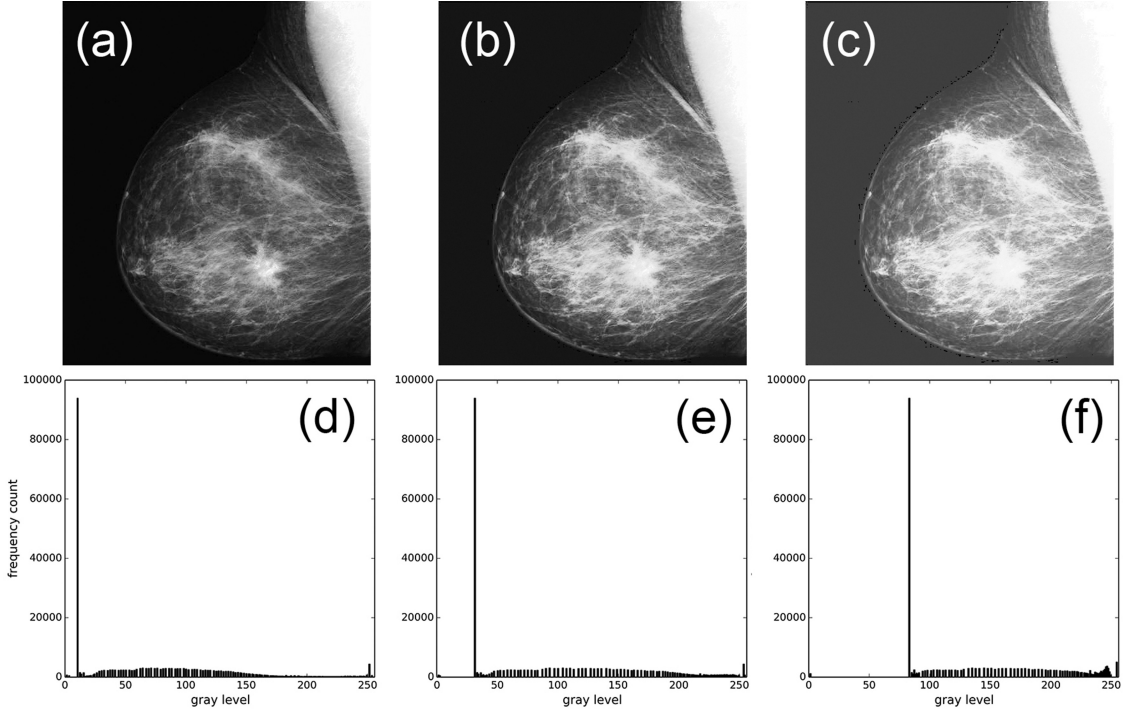


**Fig. 3:** Example of the pow-log contrast operator effect on the image of Fig. 1a. (a-c): Results for  $\beta$  equal to 3,6 and 9 respectively. (d-f): Histograms corresponding to (a-c).

where the uniform histogram  $h_u$  is approximated by  $h'_u$  which represents the logarithm of the input histogram. Figure 4 shows that the optimal value of  $\beta$  for the image from Fig. 1a is about 5.

### 2.3 Iterative Mode

The pow-log contrast enhancement operator can also be applied in an iterative mode (Iterative Pow-Log or IPL). In that case  $\beta$  is initially set to a relative small value (e.g. 3) to guarantee a conservative contrast enhancement, and the operator is repeatedly applied. This results in a moderate stepwise contrast enhancement. The Root Mean Square Error (RMSE) is used to quantify the degree of contrast enhancement between two successive iteration steps:

$$RMSE = \sqrt{\frac{1}{M \times N} \sum_{i=1}^M \sum_{j=1}^N |I^k(i,j) - I^{k+1}(i,j)|^2} \quad (4)$$

where  $I^k$  represents the image  $I$  of size  $M \times N$  pixels after  $k$  applications of the pow-log operator (i.e. the image after the  $k^{th}$  iteration step). The iteration ends when the value of RMSE drops below a small predefined threshold value.

Figure 5 shows the effect of IPL on the image from Fig. 1a. This example shows that IPL only enhances the regions of interest while the background remains nearly unaffected. The corresponding histograms (Fig. 5d-f) show that the histogram is slowly spread over the range of available grayscales during the iteration process while the spike remains in place.

Figure 6 shows that the RMSE quickly decreases after only a few iteration steps.

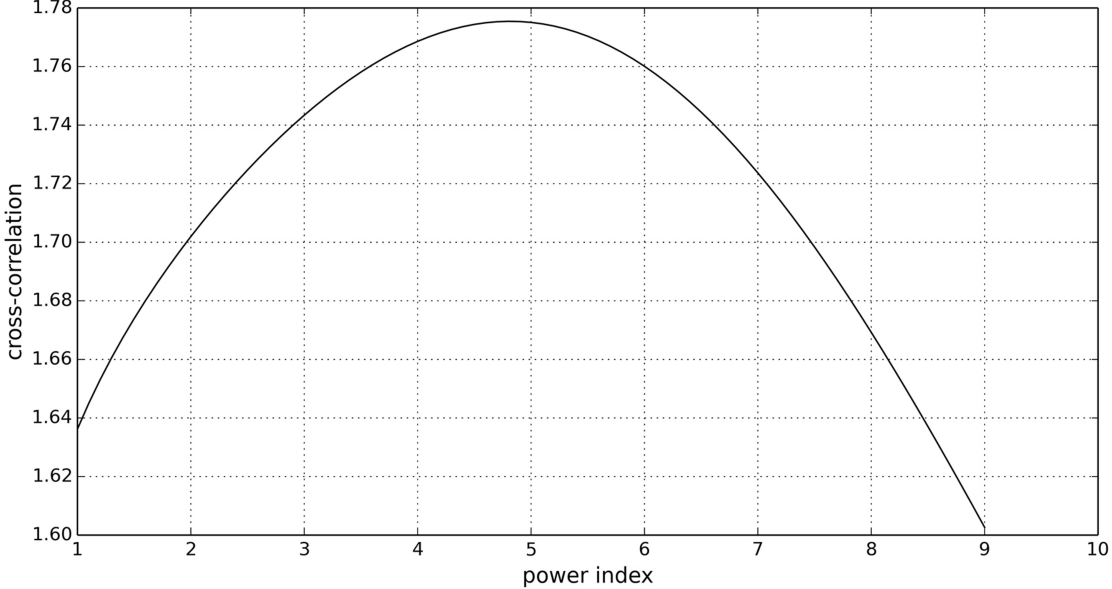


**Fig. 4:** Example of the heuristic search process to obtain the optimal value of  $\beta$  for Fig. 2a. The value of  $\beta$  is set to 1 at the start of the iteration and increases by 0.1 at each next iteration step.

Note that  $\beta$  can also be optimized at each iteration step of IPL. However, pilot studies have shown that this approach does not yield significantly different results while it does increase the computational complexity of the algorithm.

### 3. Evaluation Methods

To evaluate the effectiveness of the proposed IPL and DPL contrast enhancement methods we applied them to a set of 68 long wave IR (thermal) images representing different outdoor urban, rural and maritime scenes. The scenes include objects like people, vehicles, boats, vegetation, buildings, and clouds. Since this image set shows a large overall variation in mean image intensity and contrast, it is suitable to assess the performance of contrast enhancement algorithms under different circumstances.

Since there is currently no universally accepted image enhancement evaluation procedure, we evaluated the enhancement capability of the proposed DPL and IPL procedures both (a) through visual inspection of the results and (b) by means of two popular computational metrics (one quantifying image contrast and the other quantifying the degradation of image appearance). In addition, we investigated the time complexity of the algorithms. The results of the proposed DPL and IPL methods are also compared with the results of the widely used HE and CLAHE contrast enhancement methods.

#### 3.1 Quantitative Assessment

There is currently no universally accepted computational metric that reliably specifies both the objective and subjective (visual) validity of an image enhancement method. We therefore employ objective metrics that are frequently used in the literature to assess the effectiveness of image enhancement algorithms. One of these metrics quantifies the degree of contrast enhancement, while the other measures the visual similarity between the original input image and the enhanced result.

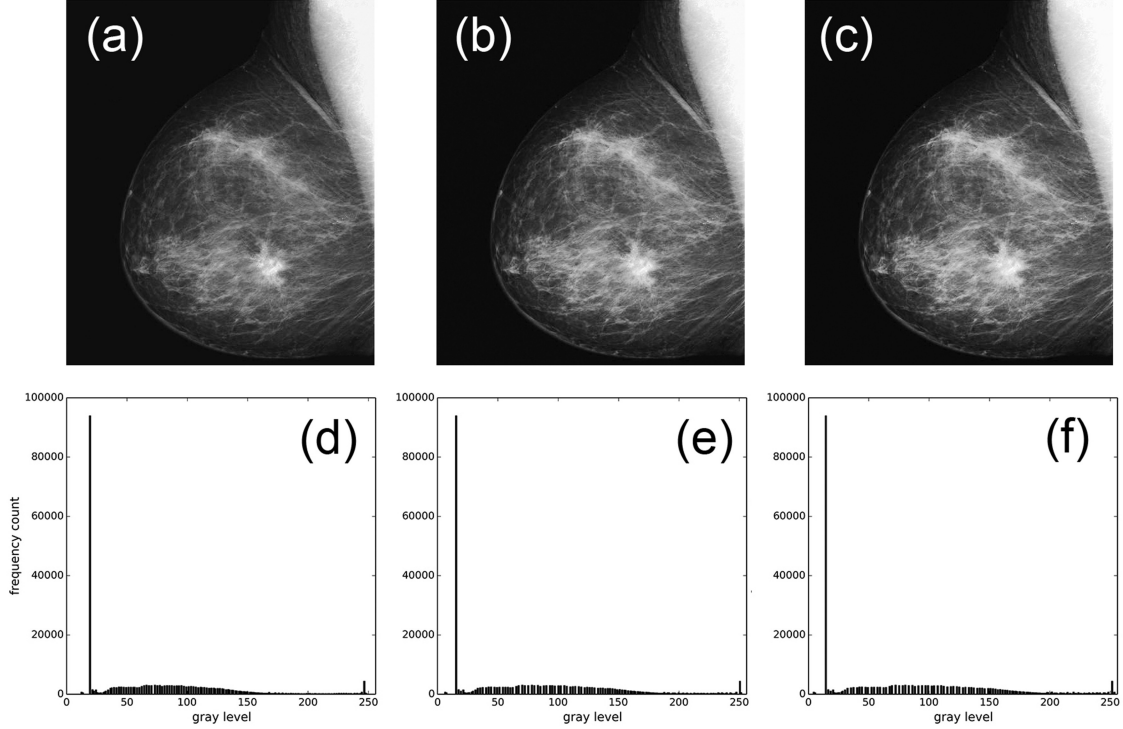


**Fig. 5:** Example of iterative contrast enhancement (IPL) of Fig. 2a. (a-c): results of steps 1,5 and 10. (d-f): histograms of (a-c).

An effective contrast enhancement method should yield results that are both significantly enhanced in contrast while their visual appearance should remain natural (i.e., the enhanced result should still resemble the input image). The metric used to quantitatively evaluate the contrast enhancement effect of the different algorithms investigated here is the root-mean-square contrast (RMSC; [9,32]), which is defined as:

$$RMSC = \sqrt{\frac{1}{M \times N} \sum_{i=1}^M \sum_{j=1}^N |I(i,j) - \bar{I}|^2} \quad (5)$$

where  $\bar{I}$  represents the average of all pixel values in the image  $I$  of size  $M \times N$  pixels. Note that the RMSC is measured by calculating the average difference between the pixel values and the overall mean of the image. Larger RMSC values indicate larger image contrast and therefore usually better enhancement. We use the RMSC metric to define a contrast enhancement factor CEF as follows:

$$CEF = \frac{RMSC(I_{out})}{RMSC(I_{in})} \quad (6)$$

where  $I_{in}$  and  $I_{out}$  denote respectively the input image and its enhanced version. The RMSC metric by its own is not sufficient to characterize the effectiveness of a contrast enhancement algorithm since its value also increases when undesirable artifacts are introduced and noise is enhanced. Hence, larger RMSC values do not necessarily indicate visual enhancement but may also signal visual degradation. To reliably evaluate the quality of the contrast

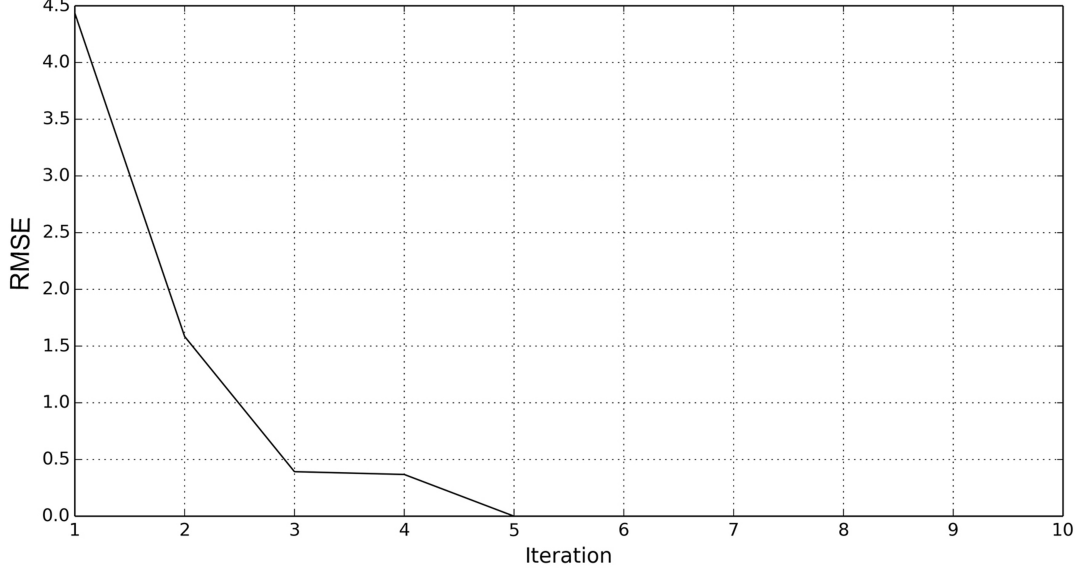


**Fig. 6:** The RMSE between two successively enhanced versions of the input image at each iteration step.

enhancement algorithms the visual appearance of the enhanced images should therefore be taken into account. This can be achieved by using the mean structural similarity metric (MSSIM; [33, 34]) which quantifies the visual similarity between the original image and its enhanced version.

The MSSIM between two images  $I_{in}$  and  $I_{out}$  of size  $M \times N$  is computed as the mean of the structural similarity index SSIM over the image support:

$$MSSIM = \sum_{i=1}^M \sum_{j=1}^N SSIM(i, j) \quad (7)$$

with

$$SSIM(i,j) =$$

$$= \frac{2\bar{I}_{in} \cdot \bar{I}_{out}}{(\bar{I}_{in})^2 + (\bar{I}_{out})^2} \cdot \frac{2\sigma_{I_{in}} \cdot \sigma_{I_{out}}}{\sigma_{I_{in}}^2 + \sigma_{I_{out}}^2} \cdot \frac{\sigma_{I_{in}, I_{out}}}{\sigma_{I_{in}} \cdot \sigma_{I_{out}}} = l(I_{in}, I_{out}) \cdot c(I_{in}, I_{out}) \cdot s(I_{in}, I_{out}) \quad (8)$$

where the mean and variances are computed over a shifting local window of size  $K \times L$  and

$$\begin{aligned} \bar{I}_{in} &= \frac{1}{K \cdot L} \sum_{k=1}^K \sum_{l=1}^L I_{in}(k, l), \quad \bar{I}_{out} = \frac{1}{K \cdot L} \sum_{k=1}^K \sum_{l=1}^L I_{out}(k, l), \\ \sigma_{I_{in}}^2 &= \frac{1}{K \cdot L - 1} \sum_{k=1}^K \sum_{l=1}^L (I_{in}(k, l) - \bar{I}_{in})^2, \\ \sigma_{I_{out}}^2 &= \frac{1}{K \cdot L - 1} \sum_{k=1}^K \sum_{l=1}^L (I_{out}(k, l) - \bar{I}_{out})^2 \end{aligned}$$

and

$$\sigma_{I_{in}, I_{out}} = \frac{1}{K \cdot L - 1} \sum_{k=1}^K \sum_{l=1}^L (I_{in}(k, l) - \bar{I}_{in}) \cdot (I_{out}(k, l) - \bar{I}_{out}).$$

The three components  $l$ ,  $c$  and  $s$  of Equation (8) measure how closely both images resemble each other in respectively mean luminance, contrast and spatial structure. Equation (8) can be reduced to

$$SSIM(i, j) = \frac{4 \cdot \sigma_{I_{in}, I_{out}} \cdot \bar{I}_{in} \cdot \bar{I}_{out}}{(\sigma_{I_{in}}^2 + \sigma_{I_{out}}^2)[(\bar{I}_{in})^2 + (\bar{I}_{out})^2]}. \quad (9)$$

The value of MSSIM varies between 0 and 1. A higher value of MSSIM indicates a higher degree of retaining structural information. This index is therefore an effective measure of the distortions and noise induced in an image as a result of any transformation. A one-way repeated measures ANOVA was conducted to determine whether the difference between the MSSIM and RMSC values for respectively DPL, IPL, HE and CLAHE on the set of 68 IR test images was significant. The statistical analyses were performed with IBM SPSS 21.0 for Windows.

### 3.2 Visual Assessment

A qualitative assessment was obtained by carefully inspecting the results of the proposed DPL and IPL contrast enhancement algorithms and by comparing their performance relative to the results of the popular HE and CLAHE enhancement techniques.

### 3.3 Computational Performance

The computational performance of the proposed algorithms is quantified by measuring the computation time required to process the individual test images. All computations were performed in MATLAB 2012a running on a PC with an Intel i5-3340M processor and 8GB RAM memory. HE was performed with the standard Matlab *histeq* function. CLAHE was performed using the standard Matlab *adaphisteq* function, dividing the images into  $8 \times 8$  tiles and limiting contrast stretching to 0.05. The maximum number of iterations for IPL was limited to 10.

## 4. Results

### 4.1 Quantitative Assessment

A one-way repeated measures ANOVA was conducted to compare the MSSIM scores and RMSC values for respectively DPL, IPL, HE and CLAHE on the set of 68 IR test images. The MSSIM scores differed significantly between all four enhancement methods (Wilks Lambda = 0.078,  $F(3, 65) = 256.475$ ,  $p < 0.0005$ , multivariate partial eta squared = 0.922). A similar analysis showed that the RMSC (and therefore the CEF) values also differed significantly between both the original input test images and all enhanced versions (Wilks Lambda = 0.194,  $F(4, 64) = 66.275$ ,  $p < 0.0005$ , multivariate partial eta squared = 0.806). Table 4.1 lists the MSSIM, RMSC and CEF values for each of the four images enhancement methods tested in this study (DPL, IPL, HE and CLAHE) for the six test images (Fig. 7-Fig. 12) discussed in Section 4.2. Also listed are the mean values (and their standard errors) of these parameters over the entire test set of 68 images.

Table 1 shows that all four methods tested in this study significantly enhance image contrast (all CEF values are significantly larger than 1). HE has the largest mean contrast enhancement factor (2.27), closely followed by IPL and DPL (1.94 and 1.80 respectively),

while CLAHE has the smallest mean CEF value (1.69). While HE has the strongest contrast enhancing effect, the results of DPL resemble the input image more closely than those of HE (DPL has a SSIM value of 0.67 versus 0.43 for HE). The mean MSSIM scores for DPL and IPL are comparable (0.67 and 0.65 respectively), whereas the mean MSSIM scores for HE and CLAHE are significantly lower (0.43 and 0.44 respectively).

Summarizing, a quantitative analysis of the capability of the tested algorithms to both enhance image contrast and retain image structure showed that the proposed DPL and IPL methods both significantly outperform HE and CLAHE on the set of IR test images used in this study. DPL retains image structure slightly better than IPL (MSSIM values of 0.67 versus 0.65), while IPL enhances contrast slightly more than DPL (CEF values of 1.94 versus 1.80).

**Table 1:** MSSIM, RMSC and CEF values for each of the four images enhancement methods tested in this study (DPL, IPL, HE and CLAHE) for six of the test images (Fig. 7-Fig. 12). Also listed are the mean values (and their standard errors) over the entire test set of 68 images.

nr	DPL			IPL		
	MSSIM	RMSC	CEF	MSSIM	RMSC	CEF
5	0.69	28.19	2.2	0.27	55.03	4.3
9	0.70	34.31	1.7	0.33	54.95	2.7
18	0.69	54.44	1.5	0.72	53.54	1.4
42	0.74	51.61	1.7	0.79	48.75	1.6
61	0.73	57.83	1.3	0.62	60.89	1.3
63	0.80	63.10	1.2	0.69	64.92	1.2
Mean (SE)	0.67 (0.01)	58.38 (1.70)	1.80 (0.09)	0.65 (0.02)	59.50 (1.61)	1.94 (0.14)

nr	HE			CLAHE		
	MSSIM	RMSC	CEF	MSSIM	RMSC	CEF
5	0.19	73.15	5.7	0.15	69.99	5.5
9	0.22	73.46	3.6	0.16	69.25	3.4
18	0.41	72.07	1.9	0.48	47.58	1.3
42	0.47	73.59	2.4	0.56	43.54	1.4
61	0.41	73.10	1.6	0.32	66.74	1.5
63	0.49	73.21	1.4	0.33	68.98	1.3
Mean (SE)	0.43 (0.02)	69.46 (1.94)	2.27 (0.21)	0.44 (0.02)	51.80 (1.82)	1.69 (0.14)

## 4.2 Visual Assessment

Figure 7a shows an example of an infrared image representing three small target (kayaks) on a sea background. The targets appear very bright against the dark sea background. DPL (Fig. 7b) enhances both the targets (notice that the upward pointing paddle held by the person in the middle kayak is clearly visible after enhancement with DPL) and the sea background (the waves are clearly visible after enhancement), without causing any artifacts. These observations are also reflected in the quantitative assessment (Table 4.1) that shows a relatively high MSSIM value (0.69) indicating that the DPL enhanced image retains the structure of the original image in combination with a relatively large CEF value (2.2) indicating a significant contrast enhancement.

IPL (Fig. 7c) enhanced image contrast somewhat more than DPL in this case ( $CEF=4.3$ ) resulting in some over-enhancement of the sea background ( $MSSIM=0.27$ ) but the targets still remain distinct. HE (Fig. 7d) has the strongest contrast enhancing effect ( $CEF=5.7$ ) but clearly over-enhances both the background and the targets ( $MSSIM=0.19$ ). As a result the middle and right target merge with the noise in the background and are no longer distinct. CLAHE (Fig. 7e) also produces an over-enhanced background with an appearance that resembles the original image even less than HE ( $MSSIM=0.15$ ).

Figure 8 is an example of enhancement comparison on an infrared image (Fig. 8a) showing a single extended target (kayak) on a sea background. DPL (Fig. 8b) enhances the background ( $CEF=1.7$ ) and some details like the wake of the vessel, the paddle held by the person and the shadow of the person on the sea surface, while the overall appearance resembles the original image quite well ( $MSSIM=0.70$ ). The same details are also enhanced by IPL (Fig. 8c) while the sea surface is enhanced somewhat more ( $CEF=2.7$ ), resulting in an overall image appearance that is less similar to the original input image ( $MSSIM=0.33$ ). HE (Fig. 8d) clearly over-enhances the overall image contrast ( $CEF=3.6$ ) giving the image an unnatural appearance and resulting in a severe degradation of the target representation ( $MSSIM=0.22$ ). CLAHE (Fig. 8e) also over-enhances the sea background ( $CEF=3.4$ ,  $MSSIM=0.16$ ) but retains the target structure, the shadows and the wake quite well.

Figure 9a is an example of an infrared image showing two persons leaving a building surrounded by vegetation. This original IR image shows a detailed representation of the persons and the doors of the building but the building itself and the surrounding vegetation are hardly visible. DPL (Fig. 9b) enhances image contrast ( $CEF=1.5$ ) so that the trees and bushes, the building and a lantern become clearly visible while the structure of the persons (e.g., darker jackets and brighter trousers) are retained ( $MSSIM=0.69$ ), as well as the structure of the doors (dark glass surrounded by brighter frames). For this image IPL (Fig. 9c) has nearly the same effect ( $CEF=1.4$ ,  $MSSIM=0.72$ ). HE (Fig. 9d) clearly over-enhances ( $CEF=1.9$ ) both the targets (no internal structure left) and the background (washout effect) resulting in an image with less detail and an unnatural appearance ( $MSSIM=0.41$ ). CLAHE (Fig. 9e) clearly enhances the overall contrast ( $CEF=1.3$ ) while retaining more of the image structure better than HE ( $MSSIM=0.48$ ). Although CLAHE also retains the articulation of the persons, information on the overall brightness level of the doors is lost. Also, parts of the sky are clearly over-enhanced resulting in spurious (noise) detail.

Figure 10a is an example of an infrared image showing a person with umbrella walking past a cabin in the woods with a building in the background. The background in the original image is clearly washed out, but the person is well articulated and the umbrella contrasts with the cabin roof in the background. DPL (Fig. 10b) clearly enhances the overall image contrast ( $CEF=1.7$ ) while retaining its appearance ( $MSSIM=0.74$ ). Note that the contrast between the umbrella and the roof is retained after DPL enhancement, while the internal structure of the cabin, the semi shrubs in the foreground, and the trees and building in the background all become more prominent. IPL (Fig. 10c) produces a similar result as DPL ( $CEF=1.6$ ,  $MSSIM=0.79$ ) but retains the articulation of the person's jacket somewhat better (notice that the folds in the jacket can still be distinguished). Although HE (Fig. 10d) enhances ( $CEF=2.4$ ) most of the background and the internal structure of the cabin, it also causes over-enhancement ( $MSSIM=0.47$ ) resulting in washout of a part of the background (trees on the left and right sides of the image) and loss of detail (the umbrella has the same graylevel as the cabin roof, and the articulation of the person's jacket is lost). In this example CLAHE (Fig. 10e) nicely enhances the overall image contrast ( $CEF=1.4$ ) without

causing too much over-enhancement ( $\text{MSSIM}=0.56$ ; only the upper part of the trees in the middle of the image are over-enhanced).

Figure 11a is an example of an infrared image showing a tank on a forest background. DPL (Fig. 11b) enhances ( $\text{CEF}=1.3$ ) both the back- and fore-ground as well as some details of the tank (the barrel, the manhole on top), while retaining the articulation of the tank's details ( $\text{MSSIM}=0.73$ ). IPL (Fig. 11c) appears to enhance ( $\text{CEF}=1.3$ ) the back- and foreground slightly more than DPL but also causes a small degree of over-enhancement over the support of the tank ( $\text{MSSIM}=0.62$ ). HE (Fig. 11d) over enhances ( $\text{CEF}=1.6$ ) both a part of the background (notice the washout effect at the left and right sides of the image) and the target itself (notice the loss of detail on the tank;  $\text{MSSIM}=0.41$ ). CLAHE (Fig. 11e) has an overall contrast enhancing effect ( $\text{CEF}=1.5$ ) but causes loss of contrast between the tank and its local background (especially on top and in front of the tank;  $\text{MSSIM}=0.32$ ).

Figure 12a is an example of an infrared image showing a truck on a forest background. DPL (Fig. 12b) enhances ( $\text{CEF}=1.2$ ) both the back- and fore-ground of the truck while retaining its internal structure ( $\text{MSSIM}=0.80$ ). The same hold for IPL (Fig. 12c) although it seems to cause a slight over-enhancement (a slight haze;  $\text{CEF}=1.2$ ) at the left side of the image ( $\text{MSSIM}=0.69$ ). HE (Fig. 12d) clearly over-enhances ( $\text{CEF}=1.4$ ) the image (washout at the left side, loss of internal detail on the truck). CLAHE (Fig. 12e) strongly enhances the overall image contrast ( $\text{CEF}=1.3$ ) but results in a loss of local contrast along the outlines of the truck making it less distinct from its local background ( $\text{MSSIM}=0.33$ ).

Summarizing, visual inspection of the results produced by the algorithms tested here showed that the proposed DPL and IPL methods outperform HE and CLAHE in most cases, in the sense that both proposed methods enhance image contrast while retaining most of the original image structure and target details and without causing spurious detail (noise, over-enhancement). In most cases DPL appears to retain image structure slightly better than IPL, while IPL enhances contrast slightly more than DPL.

### 4.3 Computational Performance

Table 4.3 lists the mean computation time (and standard error) over all 68 test images for DPL, IPL, HE and CLAHE. CLAHE is by far the computationally least efficient method. DPL is about twice as fast as IPL. Although DPL and IPL are an order of magnitude slower than HE they are still an order of magnitude faster than CLAHE. Note that no effort was made to optimize the implementation of the proposed algorithms.

**Table 2:** Mean computation time (and standard error) over all 68 test images for the new DPL and IPL methods compared with the popular HE and CLAHE contrast enhancement techniques.

Method	Mean computationtime (SE) in sec
DPL	4.7 (0.1)
IPL	9.7 (0.4)
HE	0.6 (0.1)
CLFGE	29.3 (0.6)

## 5. Conclusions

In this study we proposed a simple power-logarithm histogram modification operator to enhance IR image contrast. The algorithm combines a logarithm operator that smoothes the input image histogram while retaining the relative ordering of the original bins, with a power operator that restores the smoothed histogram to an approximation of the original input histogram. Contrast enhancement is then achieved by using the cumulative distribution

function of the resulting histogram in a standard lookup table based histogram equalization procedure.

The method is simple and independent of image content, and (unlike most existing contrast enhancement algorithms) does not suffer from the occurrence of artifacts, over-enhancement and unnatural effects in the processed images. The method can be applied both in a direct (DPL) and in an iterative (IPL) mode.

Objective (computational) and subjective (visual) evaluation studies using a wide range of different IR input images showed that both implementations of the proposed image enhancement method (DPL and IPL) significantly enhance image contrast while retaining the overall image structure and preserving the perceptibility of small details and targets. In this sense DPL and IPL both also outperformed HE and CLAHE on the set of IR test images used in this study, since these techniques introduce spurious noise and over-enhance the images in most cases resulting in image with an unnatural appearance. DPL retains image structure slightly better than IPL, while IPL enhances contrast slightly more than DPL.

We conclude that the proposed method is a robust and efficient technique for effective IR image contrast enhancement.

### Acknowledgments

Effort sponsored by the Air Force Office of Scientific Research, Air Force Material Command, USAF, under grant number FA8655-11-1-3015. The U.S. Government is authorized to reproduce and distribute reprints for Governmental purpose notwithstanding any copyright notation thereon.

### References

- [1] M. Kaur, J. Kaur, and J. Kaur, *Survey of contrast enhancement techniques based on histogram equalization*, International Journal of Advanced Computer Science and Applications, vol. 2(7), pp. 138-141, 2011.
- [2] V.A. Kotkar and S.S. Gharde, *Review of various image contrast enhancement techniques*, International Journal of Innovative Research in Science, Engineering and Technology, vol. 2(7), pp. 2786-2793, 2013.
- [3] R. Maini and H. Aggarwal, *A comprehensive review of image enhancement techniques*, Journal of Computing, vol. 2(3), pp. 8-13, 2010.
- [4] H.K. Sawant and M. Deore, *A comprehensive review of image enhancement techniques*, International Journal of Computer Technology and Electronics Engineering (IJCTEE), vol. 1(2), pp. 39-44, 2010.
- [5] T.R. Singh, O.I. Singh, Kh.M. Singh, T. Sinam, and Th.R. Singh, *Image enhancement by adaptive power-law transformations*, Bahria University Journal of Information & Communication Technology, vol. 3(1), pp. 29-37, 2010.
- [6] Y.-S. Chiu, F.-C. Cheng, and S.-C. Huang, *Efficient contrast enhancement using adaptive gamma correction and cumulative intensity distribution*, IEEE International Conference on Systems, Man, and Cybernetics (SMC 2011), IEEE, Washington, DC, USA, pp. 2946-2950, 2011.
- [7] R.C. Gonzalez and P. Wintz, *Digital Image Processing*, 3th ed., Pearson - Prentice Hall, Upper Saddle River, New Jersey, USA, 2007.
- [8] F. Branchitta, M. Diani, G. Corsini, and A. Porta, *Dynamic-range compression and contrast enhancement in infrared imaging systems*, Optical Engineering, vol. 47(7), pp. 076401-076414, 2008.
- [9] C. Zuo, Q. Chen, N. Liu, J. Ren, and X. Sui, *Display and detail enhancement for high-dynamic-range infrared images*, Optical Engineering, vol. 50(12), pp. 127401-127409, 2011.

- [10] A. Raju, G.S. Dwarakish, and D.V. Reddy, *A comparative analysis of histogram equalization based techniques for contrast enhancement and brightness preserving*, International Journal of Signal Processing, Image Processing and Pattern Recognition, vol. 6(5), pp. 353-366, 2013.
- [11] J.A. Stark, *Adaptive image contrast enhancement using generalizations of histogram equalization*, IEEE Transactions on Image Processing, vol. 9(5), pp. 889-896, 2000.
- [12] J.-Y. Kim, L.-S. Kim, and S.-H. Hwang, *An advanced contrast enhancement using partially overlapped sub-block histogram equalization*, IEEE Transactions on Circuits and Systems for Video Technology, vol. 11(4), pp. 475-484, 2001.
- [13] S.M. Pizer, E.P. Amburn, J.D. Austin, R. Cromartie, A. Geselowitz, T. Greer, B. ter Haar Romeny, J.B. Zimmerman, and K. Zuiderveld, *Adaptive histogram equalization and its variations*, Computer Vision, Graphics, and Image Processing, vol. 39(3), pp. 355-368, 1987.
- [14] K. Yeong-Taeg, *Contrast enhancement using brightness preserving bi-histogram equalization*, IEEE Transactions on Consumer Electronics, vol. 43(1), pp. 1-8, 1997.
- [15] W. Yu, C. Qian, and Z. Baomin, *Image enhancement based on equal area dualistic sub-image histogram equalization method*, IEEE Transactions on Consumer Electronics, vol. 45(1), pp. 68-75, 1999.
- [16] C. Wang and Z. Ye, *Brightness preserving histogram equalization with maximum entropy: a variational perspective*, IEEE Transactions on Consumer Electronics, vol. 51(4), pp. 1326-1334, 2005.
- [17] F. Lamberti, B. Montrucchio, and A. Sanna, *CMBFHE: a novel contrast enhancement technique based on cascaded multistep binomial filtering histogram equalization*, IEEE Transactions on Consumer Electronics, vol. 52(3), pp. 966-974, 2006.
- [18] K.S. Sim, C.P. Tso, and Y.Y. Tan, *Recursive sub-image histogram equalization applied to gray scale images*, Pattern Recognition Letters, vol. 28(10), pp. 1209-1221, 2007.
- [19] M. Kim and M.G. Chung, *Recursively separated and weighted histogram equalization for brightness preservation and contrast enhancement*, IEEE Transactions on Consumer Electronics, vol. 54(3), pp. 1389-1397, 2008.
- [20] C. Wang, J. Peng, and Z. Ye, *Flattest histogram specification with accurate brightness preservation*, IET Image Processing, vol. 2(5), pp. 249-262, 2008.
- [21] Z.G. Wang, Z.H. Liang, and C.L. Liu, *A real-time image processor with combining dynamic contrast ratio enhancement and inverse gamma correction for PDP*, Displays, vol. 30(3), pp. 133-139, 2009.
- [22] Z. Chen, B.R. Abidi, D.L. Page, and M.A. Abidi, *Gray-level grouping (GLG): an automatic method for optimized image contrast enhancement - part I: the basic method*, IEEE Transactions on Image Processing, vol. 15(8), pp. 2290-2302, 2006.
- [23] Z. Chen, B.R. Abidi, D.L. Page, and M.A. Abidi, *Gray-level grouping (GLG): an automatic method for optimized image contrast enhancement - part II: the variations*, IEEE Transactions on Image Processing, vol. 15(8), pp. 2303-2314, 2006.
- [24] T. Arici, S. Dikbas, and Y. Altunbasak, *A histogram modification framework and Its application for image contrast enhancement*, IEEE Transactions on Image Processing, vol. 18(9), pp. 1921-1935, 2009.
- [25] S. Lee, *Content-based image enhancement in the compressed domain based on multi-scale a-rooting algorithm*, Pattern Recognition Letters, vol. 27(10), pp. 1054-1066, 2006.
- [26] S. Dippel, M. Stahl, R. Wiemker, and T. Blaffert, *Multiscale contrast enhancement for radiographies: Laplacian pyramid versus fast wavelet transform*, IEEE Transactions on Medical Imaging, vol. 21(4), pp. 343-353, 2002.
- [27] B.j. Wang, S.q. Liu, Q. Li, and H.X. Zhou, *A real-time contrast enhancement algorithm for infrared images based on plateau histogram*, Infrared Physics & Technology, vol. 48(1), pp. 77-82, 2006.
- [28] K. Liang, Y. Ma, Y. Xie, B. Zhou, and R. Wang, *A new adaptive contrast enhancement algorithm for infrared images based on double plateaus histogram equalization*, Infrared Physics & Technology, vol. 55(4), pp. 309-315, 2012.
- [29] W. Zhao, Z. Xu, J. Zhao, F. Zhao, and X. Han, *Variational infrared image enhancement based on adaptive dual-threshold gradient field equalization*, Infrared Physics & Technology, vol. 66(0), pp. 152-159, 2014.

- [30] X. Bai, F. Zhou, and B. Xue, *Infrared image enhancement through contrast enhancement by using multiscale new top-hat transform*, Infrared Physics & Technology, vol. 54(2), pp. 61-69, 2011.
- [31] J. Zhao, Y. Chen, H. Feng, Z. Xu, and Q. Li, *Infrared image enhancement through saliency feature analysis based on multi-scale decomposition*, Infrared Physics & Technology, vol. 62(0), pp. 86-93, 2014.
- [32] E. Peli, *Contrast in complex images*, Journal of the Optical Society of America A, vol. 7(10), pp. 2032-2040, 1990.
- [33] Z. Wang and A.C. Bovik, *A universal image quality index*, IEEE Signal Processing Letters, vol. 9(3), pp. 81-84, 2002.
- [34] Z. Wang, A.C. Bovik, H.R. Sheikh, and E.P. Simoncelli, *Image quality assessment: from error visibility to structural similarity*, IEEE Transactions on Image Processing, vol. 13(4), pp. 600-612, 2004.

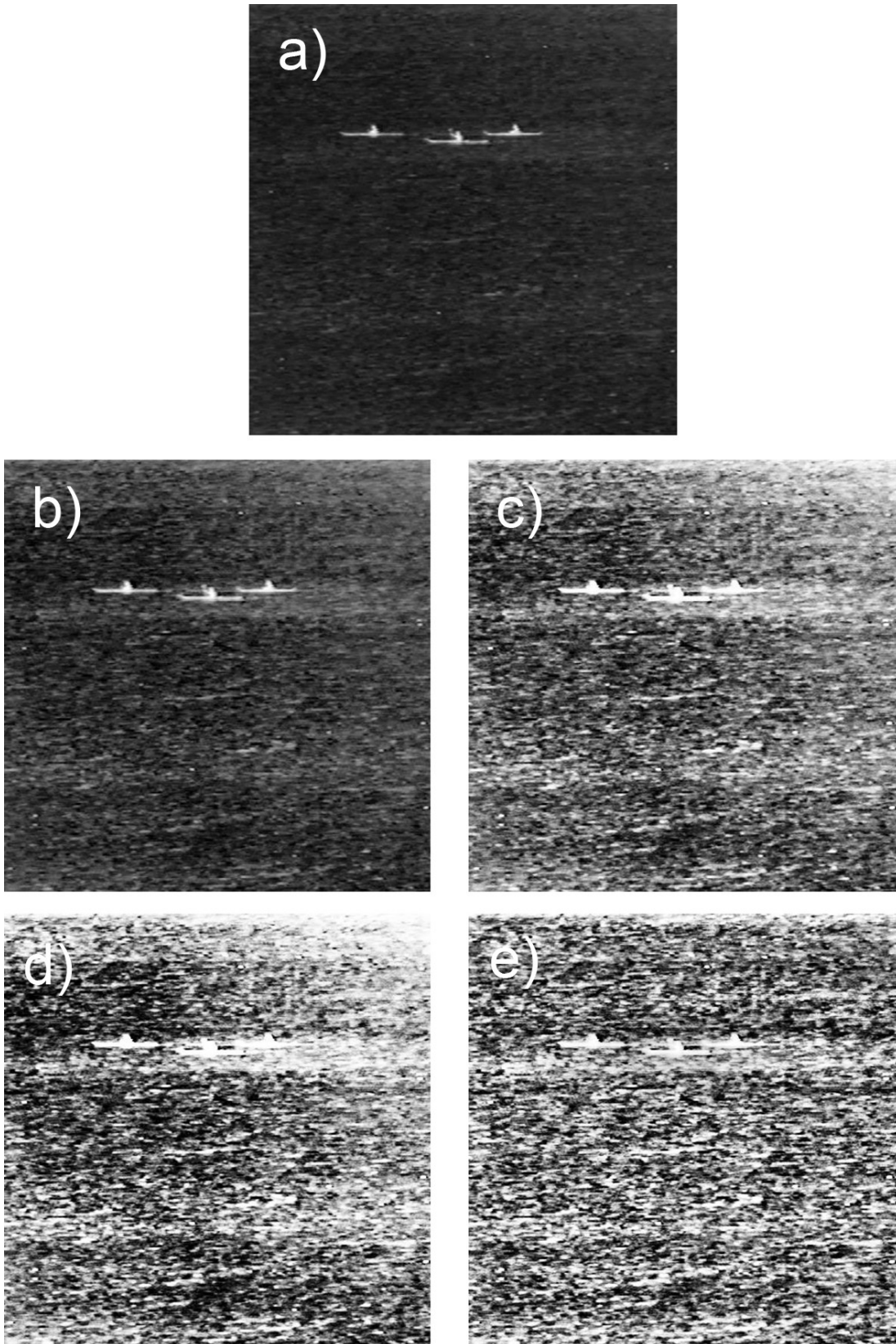


**Fig. 7:** Example of enhancement comparison on an infrared image showing three small target (kayaks) on a sea background. (a) Original IR image, (b) result of DPL, (c) result of IPL, (d) result of HE, and (e) result of CLAHE.

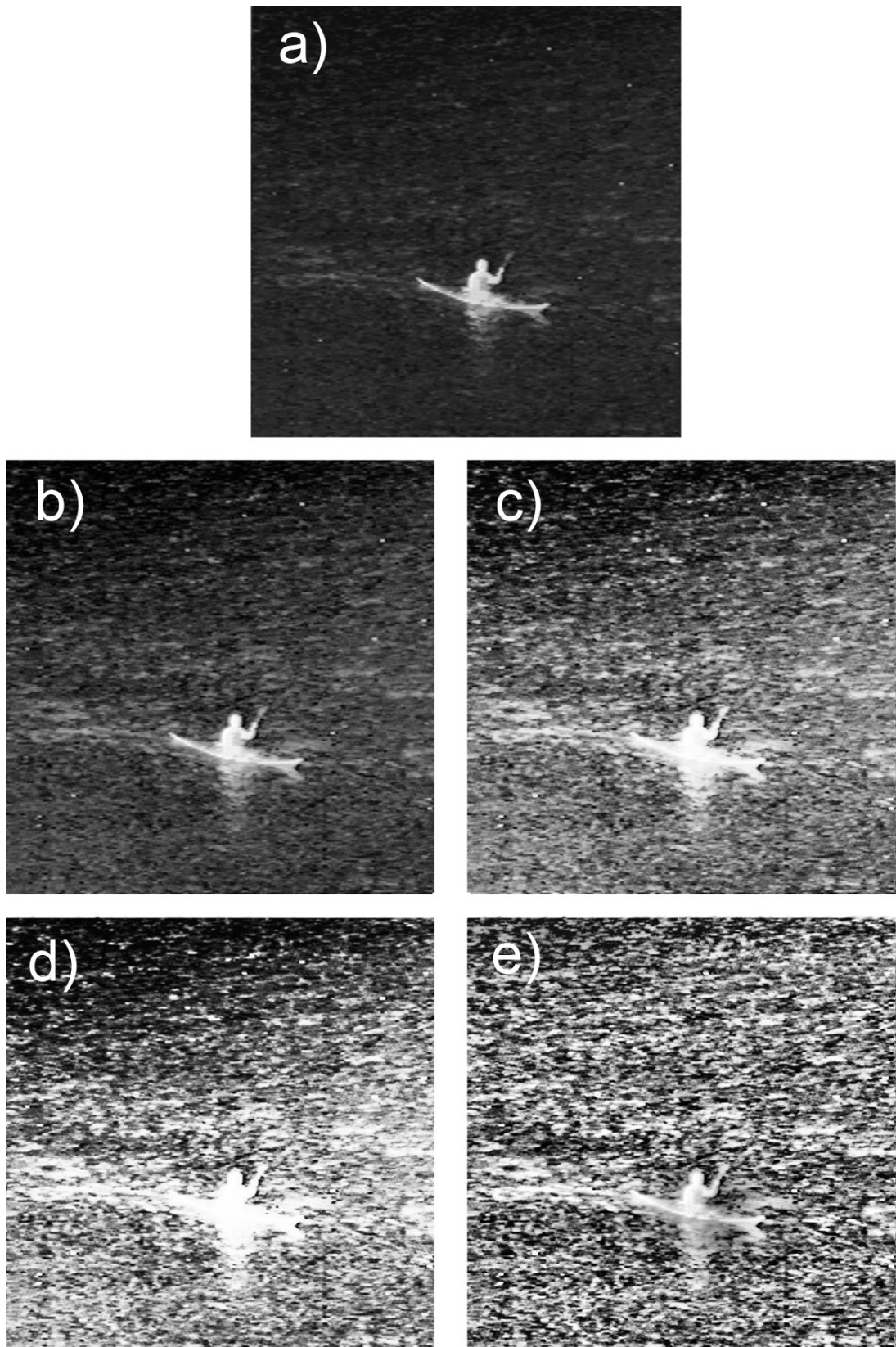


**Fig. 8:** Example of enhancement comparison on an infrared image showing a target (kayak) on a sea background. (a) Original IR image, (b) result of DPL, (c) result of IPL, (d) result of HE, and (e) result of CLAHE.

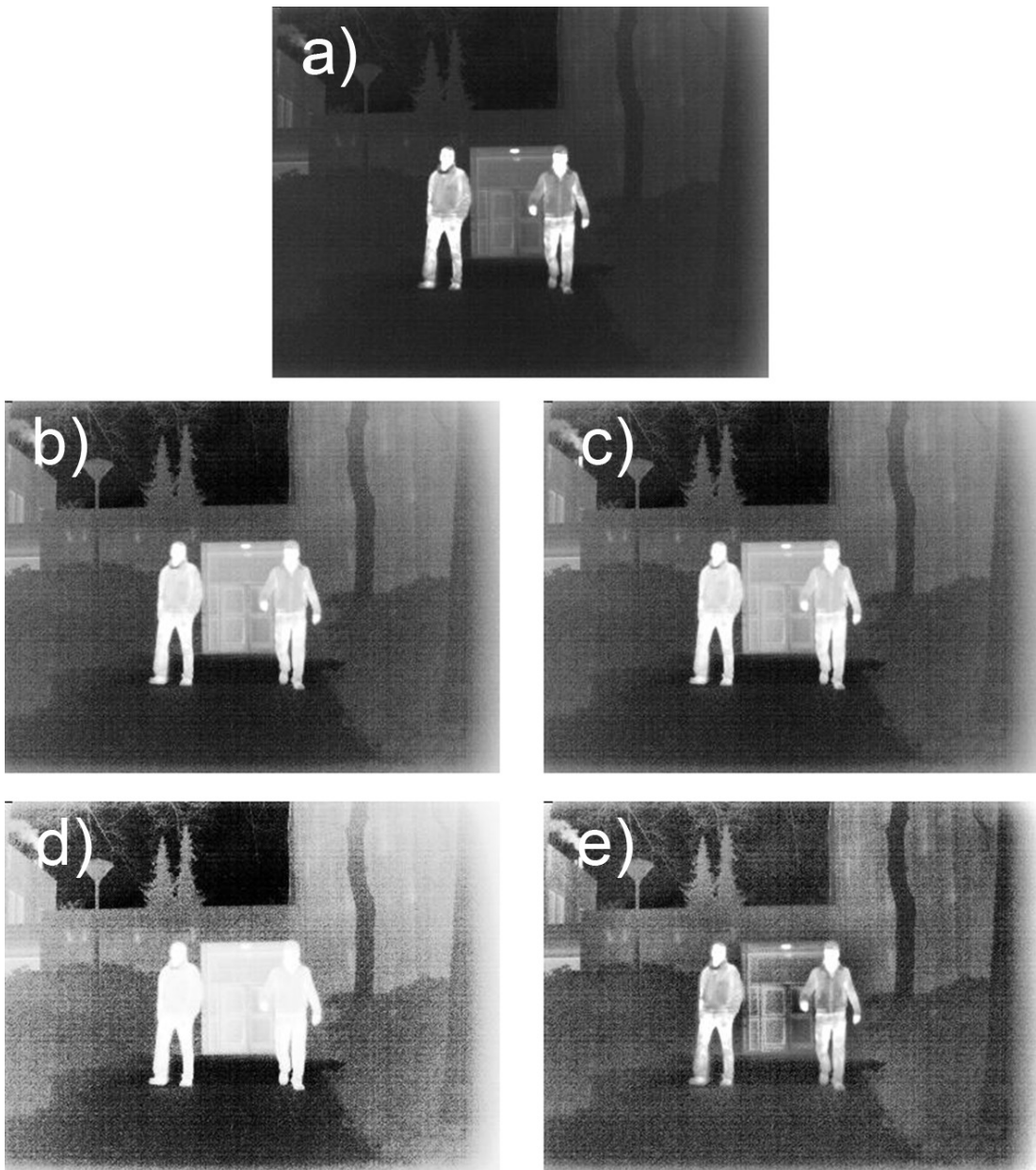


**Fig. 9:** Example of enhancement comparison on an infrared image showing two persons leaving a building surrounded by vegetation. (a) Original IR image, (b) result of DPL, (c) result of IPL, (d) result of HE, and (e) result of CLAHE.

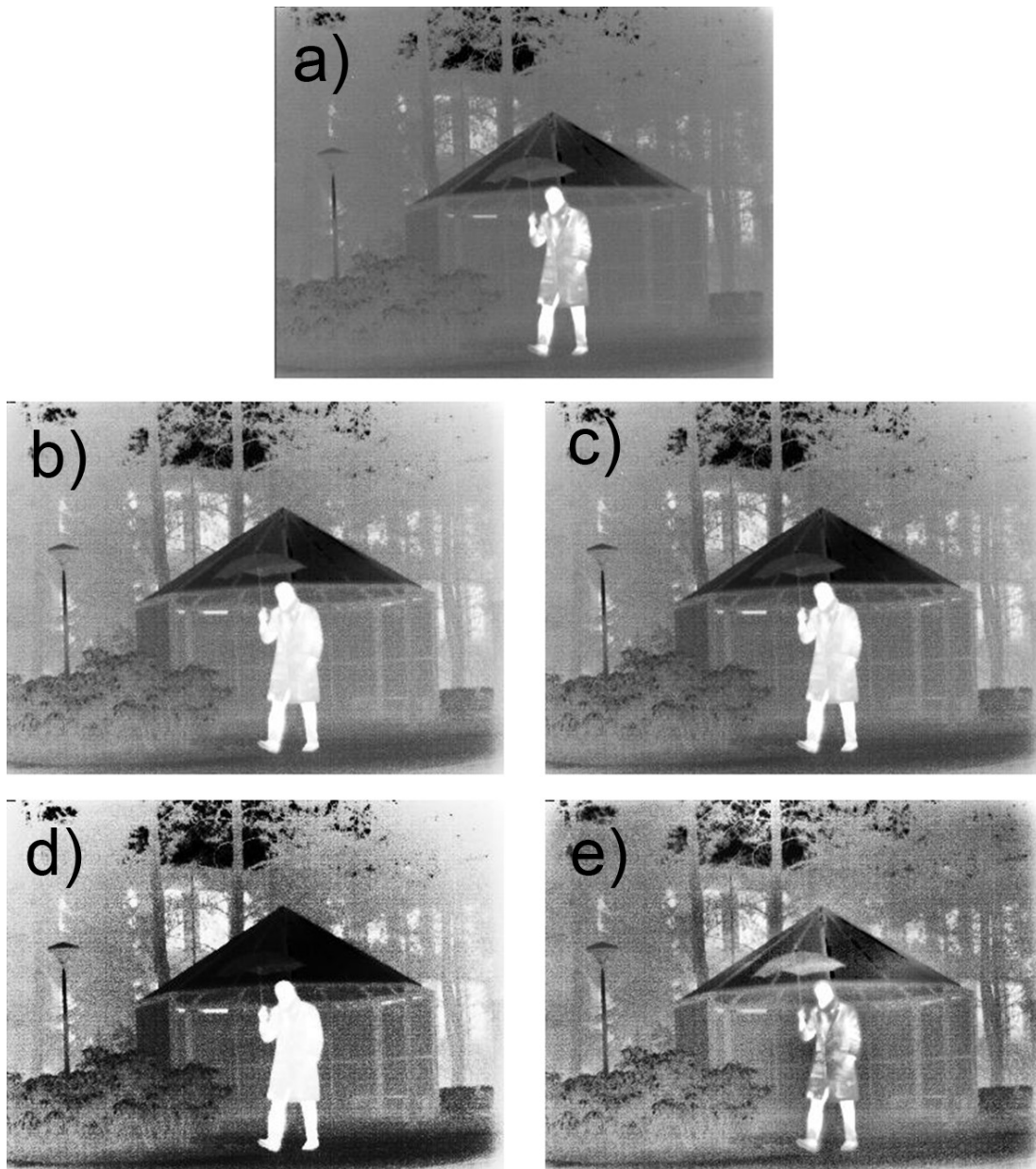


**Fig. 10:** Example of enhancement comparison on an infrared image showing a man with umbrella walking past a cabin in the woods with a building in the background. (a) Original IR image, (b) result of DPL, (c) result of IPL, (d) result of HE, and (e) result of CLAHE.

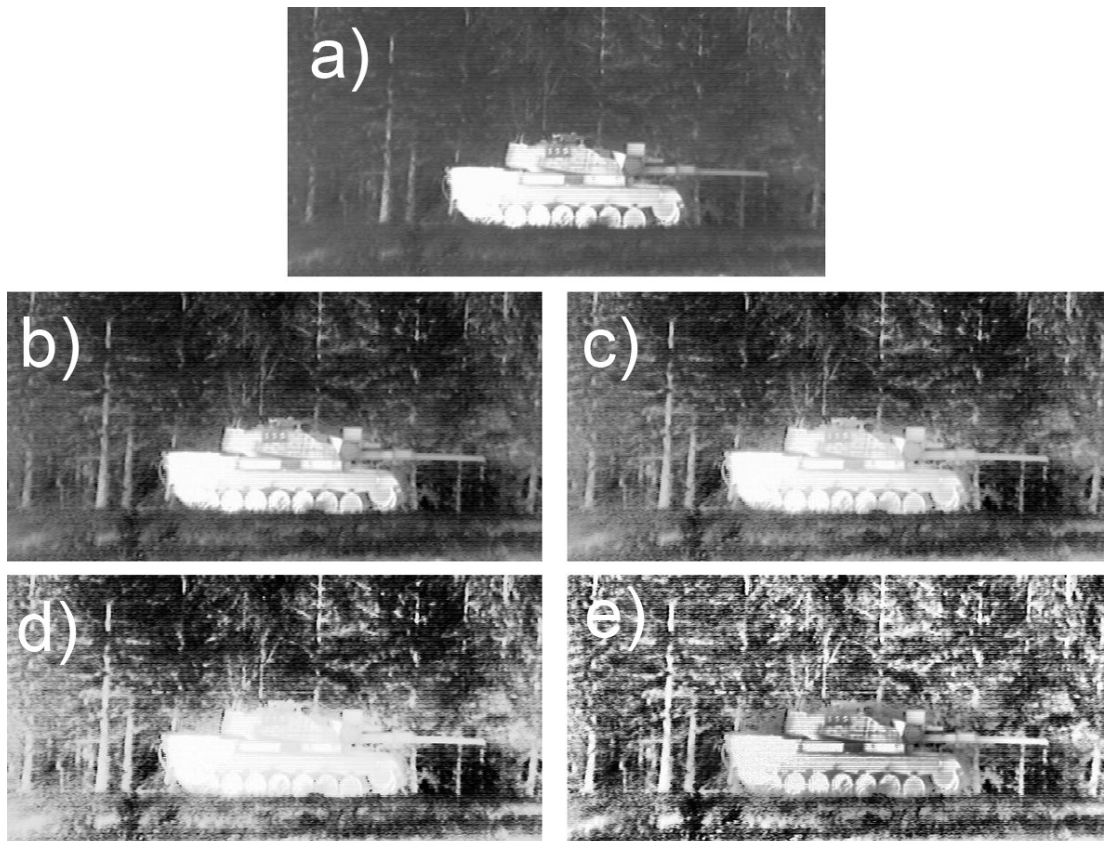


**Fig. 11:** Example of enhancement comparison on an infrared image showing a tank on a forest background. (a) Original IR image, (b) result of DPL, (c) result of IPL, (d) result of HE, and (e) result of CLAHE.

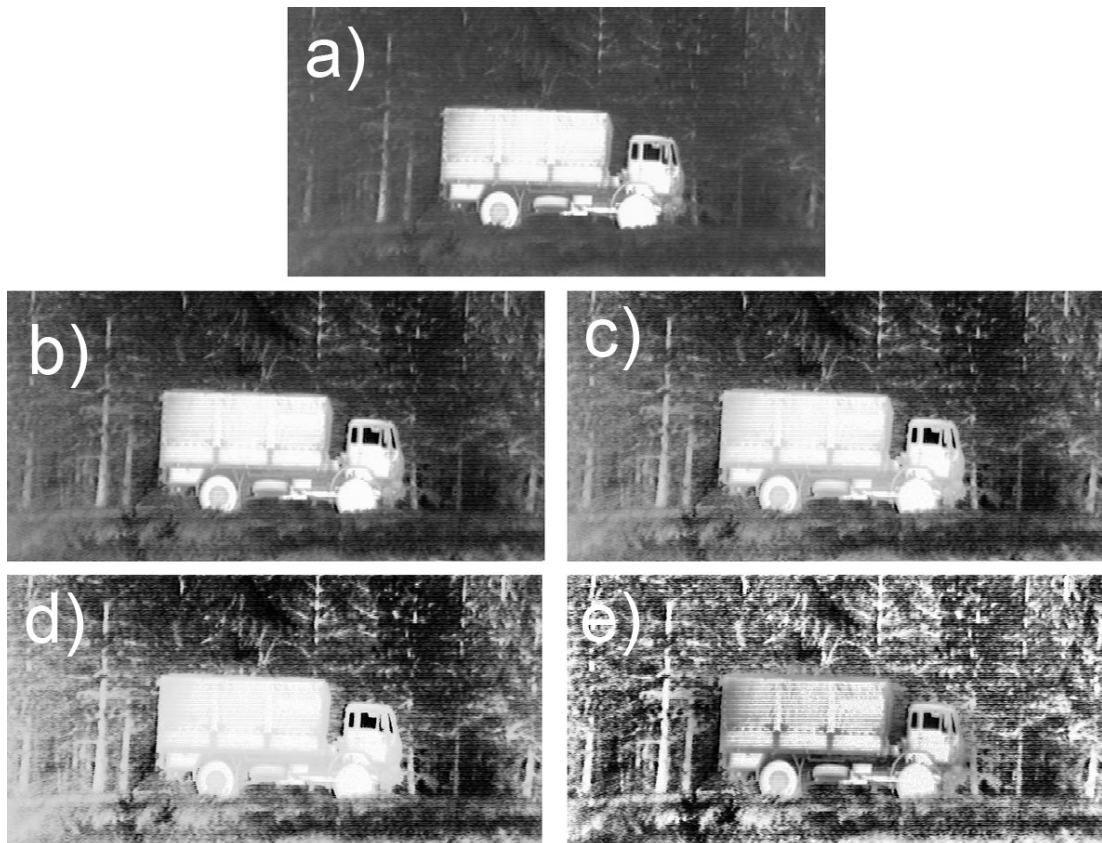


**Fig. 12:** Example of enhancement comparison on an infrared image showing a truck on a forest background.  
(a) Original IR image, (b) result of DPL, (c) result of IPL, (d) result of HE, and (e) result of CLAHE.